J. exp. Biol. **112**, 129–145 (1984)
Printed in Great Britain © *The Company of Biologists Limited 1984*

RELATIONSHIPS BETWEEN NEURONAL STRUCTURE AND FUNCTION

BY JOHN P. MILLER AND GWEN A. JACOBS

Department of Zoology, University of California, Berkeley and
Department of Biology, State University of New York, Albany, U.S.A.

SUMMARY

The geometry and electrical properties of a neurone determine how synaptic inputs and endogenously generated currents are integrated and transformed into the signals it transmits to other cells. The dependence of neuronal integration upon dendritic geometry has been studied extensively over the last three decades, both by experimentalists and by theoreticians. We review some of the general principles that have emerged from this work, and summarize recent studies that serve to illustrate these principles. The discussion is organized around the analysis of neuronal structure at three different levels. At the 'macroscopic' level, we show how the dendritic branching structure of an identified interneurone in the cricket cercal afferent system determines the directional sensitivity within its receptive field. At the 'microscopic' level, we illustrate the dependence of synaptic efficacy upon dendritic length, and demonstrate a very surprising result: that the extension (or 'growth') of a dendrite out beyond the point of a synaptic contact can increase the efficacy of that synapse. At the 'ultrastructural' level, we show how the structural and electrical properties of dendritic spines might have profound effects upon synaptic integration.

INTRODUCTION

It is a fundamental principle of neurobiology that the function of a neurone is dependent upon its structure. The structure determines, to a large extent, how the synaptic inputs and endogenously generated currents of neurones are 'integrated' and transformed into a 'meaningful' output to other neurones, muscles or effector organs. This functional dependence upon neuronal structure is manifest at three levels within a nerve cell: the 'macroscopic', 'microscopic' and 'ultrastructural'. By 'macroscopic' structure, we mean the overall shape of a neurone, how many dendritic and axonal branches it has, and where in the nervous system those branches are located. By 'microscopic' structure, we mean the shape, length, diameter and branching points of the individual branches. By 'ultrastructure', we mean the shapes of the neurites near the points where synaptic contacts are located, the 'local' contours, dendritic spines and varicosities.

The dependence of neuronal integration upon dendritic geometry at each of these three levels has been studied extensively over the last three decades, both analytically

Key words: Synaptic efficacy, neuronal modelling, laser microsurgery.

and through the use of computer models. Due to the work of Rall, Jack, Redman Shepherd and many others, we have all developed a common, quantitative conventional wisdom about the relationships between neuronal structure and function. In addition, recent advances in single cell staining techniques now allow experimenters to take morphological measurements of cells from which electrophysiological recordings have been obtained. Together, these theoretical and experimental studies have given us the tools we need to ask and answer very precise questions about neuronal form and function. It is the purpose of this paper to discuss the relationships between neuronal structure and function at each of the three levels listed above, by presenting examples of recent work which illustrate the use of new experimental and computer modelling techniques.

At the 'macroscopic' level, we show how the dendritic branching structure of an interneurone in the cricket cercal afferent system determines the directional sensitivity within its receptive field. This example also demonstrates the use of a new technique we have developed which allows the experimenter to modify the structure of a cell while its activity is being monitored. The technique utilizes a laser microbeam to photoinactivate individual identified dendrites. This section also demonstrates how a computer model of this identified neurone was used to address questions that could not be answered through direct physiological experiments.

At the 'microscopic' and 'ultrastructural' levels we summarize recent theoretical modelling studies that one of us (JPM) has carried out in collaboration with Drs Wilfrid Rall and John Rinzel. At the 'microscopic' level we illustrate the dependence of synaptic efficacy upon dendritic length, and demonstrate a very surprising result. We show that the extension (or 'growth') of a dendrite out beyond the point of a synaptic contact can increase the efficacy of that synapse. At the 'ultrastructural' level we show how the structural and electrical parameters of dendritic spines might have profound effects upon synaptic integration. In particular, if the membrane on the head of a spine is capable of generating an action potential, a spine may act as a powerful 'amplifier' of synaptic efficacy.

MACROSCOPIC STRUCTURE

The shape of a neurone, in terms of the number and position of its dendritic branches, determines both the inputs it receives as well as its postsynaptic targets. The 'function' of a neurone is dictated by its connectivity to other ones and thus is tightly linked to its structure at this macroscopic level. Many types of neurones have dendrites that project to distinct regions of the nervous system and can receive different synaptic inputs specific for each dendrite. An excellent example of this type of neurone is found in the cricket cercal afferent system. Anatomical studies reviewed by Murphey, Walthall & Jacobs in this volume describe how the dendrites of wind-sensitive interneurones overlap with different classes of sensory afferents. Each class of sensory afferent responds optimally to a different wind direction (Palka, Levine & Schubiger, 1977) and occupies a distinct region of neuropile (Bacon & Murphey, 1984). These studies suggest that the receptive fields of the wind-sensitive interneurones are determined by the position of their dendrites with respect to the different classes of sensory afferents. In this section we summarize experiments which test this

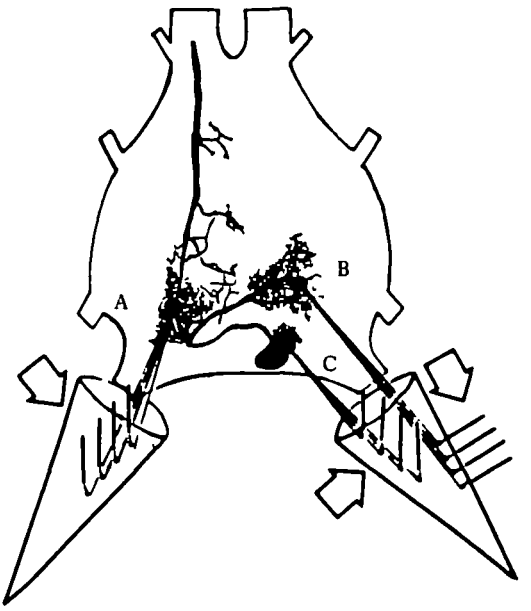

Fig. 1. *Camera lucida* drawing of interneurone 10-3 in the terminal abdominal ganglion. Three classes of sensory afferents associated with filiform hairs on the cerci (represented as cones at the rear of the ganglion) overlap with the three dendrites labelled A, B and C. Each class responds to a different optimal wind direction indicated by arrows pointing at the hairs.

hypothesis directly for an identified interneurone. We demonstrate that this interneurone receives different inputs specific to each dendrite and that it sums these inputs in different combinations to shape its receptive field.

Fig. 1 is a *camera lucida* drawing of the identified sensory interneurone, '10-3' that we have used in our experiments. It has three separate dendritic regions in the last abdominal ganglion of the cricket nervous system. Based on anatomical observations described in detail by Murphey, Walthall & Jacobs (this volume), each dendrite is known to overlap with a separate class of sensory afferent which is sensitive to a different wind direction. This is shown schematically in Fig. 1. These sensory neurones innervate filiform hairs that cover the surface of two sensory appendages called cerci at the rear of the animal. The hairs are lodged in sockets that constrain their movements to a single plane (Palka *et al.* 1977). The sensory neurone responds only when the associated hair is deflected in one direction (Tobias & Murphey, 1979). Puffing wind at the cerci from different directions therefore selectively activates different classes of sensory afferents, and thus provides a means of testing whether the receptive field of 10-3 fits the anatomical predictions suggested by Murphey and his co-workers.

We recorded intracellularly from the soma of 10-3 while calibrated wind puffs were delivered at the cerci by a device that could be moved 360° around the body. We could predict which dendrites would be activated by observing the movements of the hairs at each stimulus orientation. Note that some wind positions activate all three classes of hairs and subsequently all three dendrites, whereas other positions activate either one or none of the dendrites. At each stimulus position the response of the cell to five wind puffs was averaged. The area under the response was measured for the first

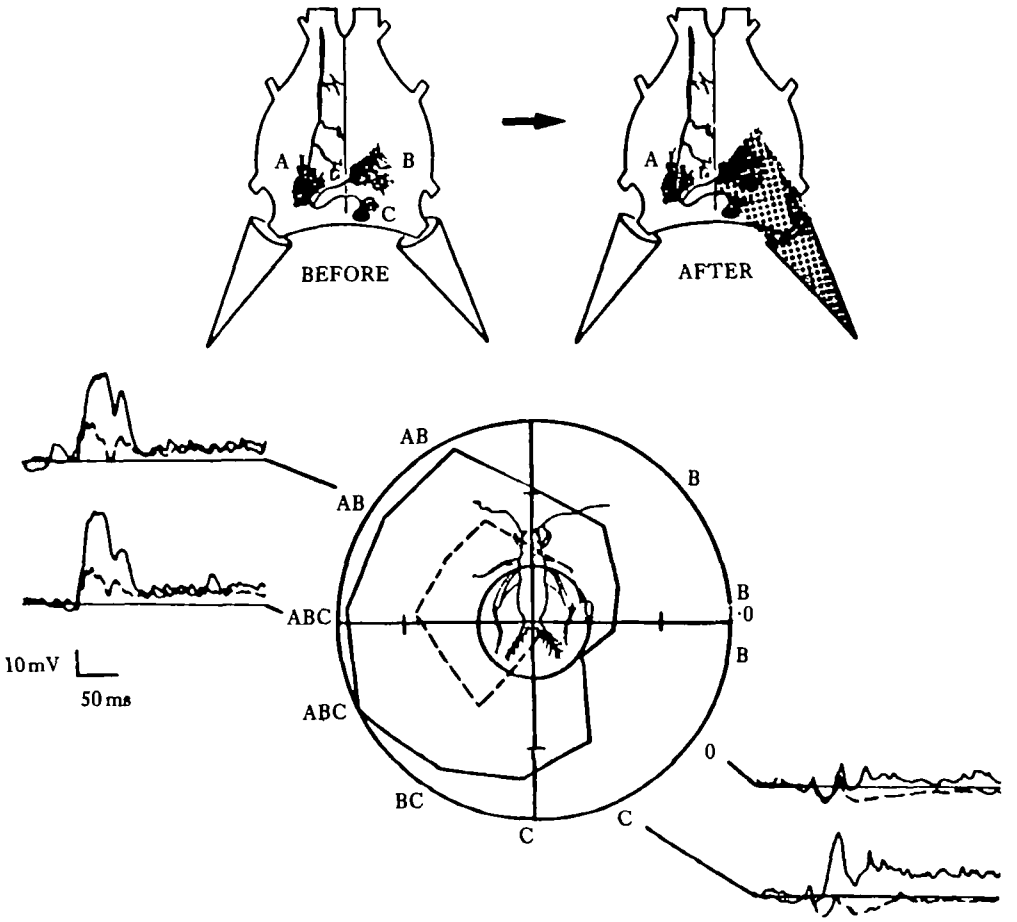

Fig. 2. Directional sensitivity of 10-3 before and after covering one cercus. The responses of it to five wind puffs at each position were averaged and the area was measured with respect to the baseline. These values were normalized to the maximum and plotted according to wind position. The outer circle indicates the maximum normalized area 1·0, and the small inner circle represents 0·0. Values inside this inner circle indicate inhibitory responses. The letters around the perimeter of the graph indicate which dendrites should be activated by wind from that direction. For example AB indicates that two afferent classes that should activate dendrites A and B are stimulated from this position. The outer solid line represents the receptive field when all inputs were intact (upper left cartoon). The inner dashed line represents the receptive field after the right cercus had been covered (the stippling in the upper right cartoon). Sample records from the cell before (solid traces) and after (dashed traces) covering the right cercus are shown superimposed at four positions around the curve.

100 ms after stimulus onset and plotted as a function of wind position. The solid line in Fig. 2 represents the receptive field and fits the anatomical predictions quite well. The cell was directionally tuned to wind directed at the front and left side of the body which corresponds to the sum of optimal wind directions for the three classes of afferents that overlap with 10-3.

Since each dendrite overlaps with a set of afferents that respond maximally to a different wind direction, each should exhibit its own directional sensitivity. Two different experiments were devised to test this. In the first, inputs onto two dendrites (B, C) were selectively blocked and the response to remaining inputs was measured

This blockage was achieved by covering the right cercus with Vaseline, which immobilizes the hairs and silences all the afferents that project to the right side of the ganglion. The inner dashed line in Fig. 2 represents the response of 10-3 to the remaining inputs. As predicted by the anatomy, the maximum response from 10-3 was observed for wind directed at the lateral face of the cercus, which is the optimal stimulus for afferents that overlap with dendrite A.

The most straightforward interpretation of these results is that the inner dashed line results solely from excitatory inputs onto dendrite A. However, we recorded inhibitory responses in this cell to wind stimuli at several other positions. These stimuli activate afferents that do not overlap with dendrite A and thus must be activating a polysynaptic pathway. The presence of these inhibitory pathways which have been identified in this (Levine & Murphey, 1980) and other analogous systems (Reichert, Plummer & Wine, 1983) clouds this simple interpretation.

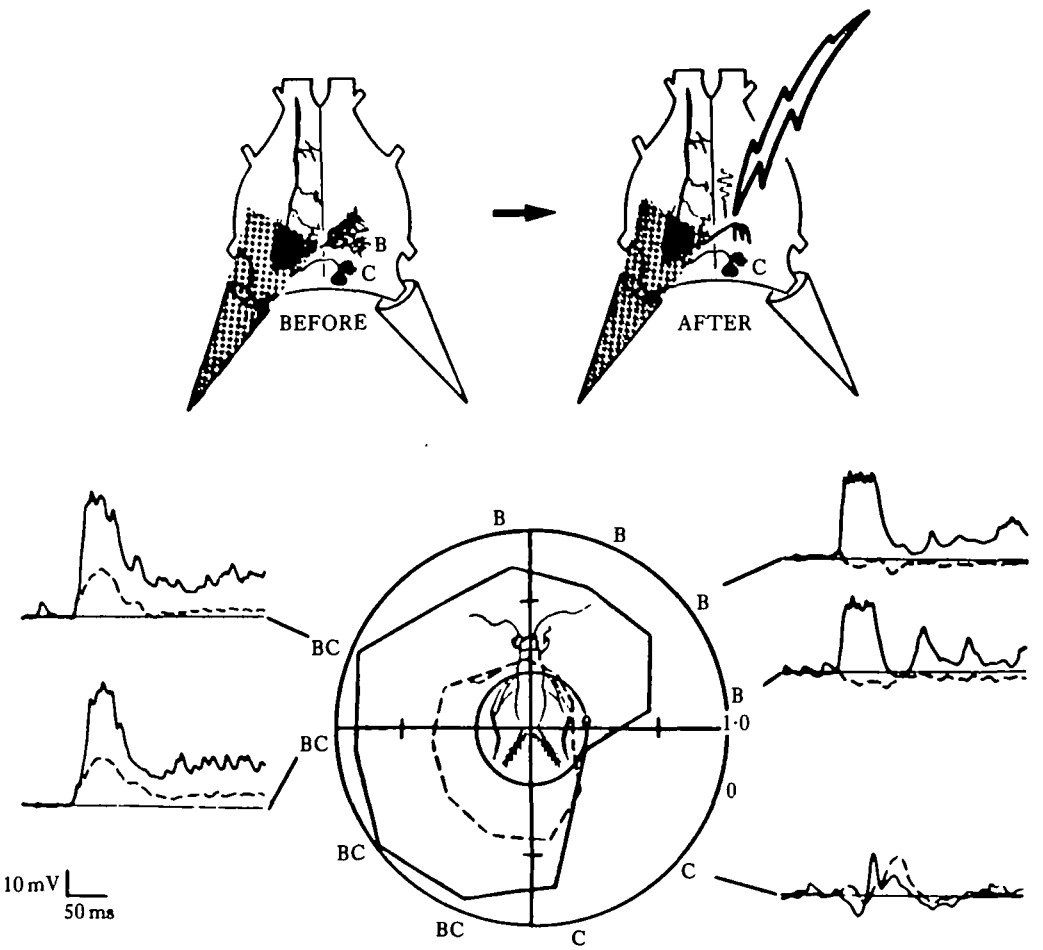

Fig. 3. Photoinactivation of a single dendrite modified the receptive field of 10-3. Receptive fields of 10-3 before (solid line) and after (dashed line) photoinactivating dendrite B were measured and plotted as in Fig. 2. The left cercus was covered with Vaseline during all measurements. Sample records before (solid traces) and after (dashed traces) photoinactivation are shown at five different positions.

In a second set of experiments a single identified dendrite was 'excised' from 10-3 *in situ*, with a laser microbeam. This technique provides a direct test of whether that dendrite receives a specific directional input and eliminates the possibility of it receiving polysynaptic input from other afferents. A modification of the dye-sensitized photoinactivation technique devised by Miller & Selverston (1979) was used to ablate dendrite B of 10-3 (Fig. 3). The cell was filled with Lucifer Yellow and the dendrite illuminated with a spot of intense blue light, using a helium-cadmium laser directed through the optics of a stereo dissecting microscope as the light source. The microbeam could be focused to a spot of about 30 μm and allowed this dendrite to be inactivated without damaging the rest of the cell. In the experiment in Fig. 3 the left cercus was covered with Vaseline to block input onto dendrite A, leaving only inputs to dendrites B and C intact. A control receptive field was measured and plotted in the outer solid line which represents the summed inputs to dendrites B and C. Dendrite B was then inactivated with the laser and the receptive field was again measured and plotted (inner dashed line). The response of this modified 10-3 was maximally sensitive to wind directed at the medial face of the right cercus which indeed is the optimal stimulus for the remaining dendrite C. Wind directed at the front of the animal, the optimal stimulus for dendrite B, produced a negligible response. At positions which activate both dendrites B and C, the response was decreased by about half, which suggests that the inactivation was limited to the B dendrite and that inputs to dendrite C were still effective. In addition, responses to stimuli which should activate only the C dendrite were not changed in amplitude. This experiment reveals the directional sensitivity of dendrite C (dashed line) and by subtraction that of dendrite B. It also proves that the B dendrite receives input from a select class of afferents that respond to wind from the front of the animal, as predicted by the anatomy.

In summary, both of the experiments provide evidence that supports the idea that the receptive field of this identified interneurone consists of contributions of specific directional inputs to each of its dendrites. The overall directional sensitivity is therefore determined by the position of its dendrites within the central nervous system.

The inherent limitations of the available recording techniques make a more complete analysis of this cell impossible. The main problem is that reliable recordings can only be obtained from the cell body. However, it is the voltage fluctuations at the spike initiating zone (SIZ) that we hope to understand and characterize, since it is these that determine its firing rate. In other words, the SIZ is where the inputs onto all of the dendrites are translated into the relevant output to higher centres.

Since we could neither locate nor record from the SIZ of 10-3 we took an alternative approach. We developed a compartmental computer model and 'asked' the model two specific questions; (1) where is the SIZ and (2) what would be the attenuation of synaptic inputs onto the different dendrites as measured at the SIZ? All structural parameters for the model (i.e. lengths and diameters of dendritic segments between branch points or between significant changes in diameter) were measured from serial sections of a 10-3 cell that had been filled with cobalt and intensified with silver (Bacon & Altman, 1977). These measurements were corrected for the shrinkage artefacts caused by the histological preparation. The model was assembled using 80 segmental compartments to represent these dendritic segments. The methods for modelling the structural and electrical properties of neurones (in this and in all other studies

summarized in this chapter) were identical to those described by Lev-tov, Miller, Burke & Rall (1983). The passive electrical parameters for these compartments (membrane capacitance, Cm, cytoplasmic resistivity, Ri, and membrane resistivity, Rm) were assumed to be uniform throughout the cell. Values for Cm and Ri were set at 1 μF cm^{-2} and 70 Ωcm respectively (for a summary of reported values from many preparations, see Rall, 1977).

Values of Rm reported for other insect neurones may not necessarily be applicable to 10-3. Therefore, we used the model to calculate the most reasonable value for Rm by re-calculating iteratively the input resistance (Rin) of the model for different values of Rm. An Rm value of 10 000 Ωcm^2 yielded an Rin of 11 MΩ, which was the value measured from the cell body of the neurone used for the anatomical reconstruction. To locate the most likely site of spike initiation, we took a similar iterative approach by programming a special subroutine that could control the voltage of any dendritic compartment of the model. This subroutine was set to generate a voltage transient that displayed the time course of a real, overshooting action potential. We could 'connect' this 'spike-initiating' routine to any compartment of the model, and calculate what the attenuated spike would look like in the cell body. When the SIZ was in the compartment corresponding to the position indicated in Fig. 4, the amplitude and time course of the attenuated spikes calculated at the model soma matched those of recorded action potentials. If the spikes were initiated further from or closer to the model soma, the attenuated spikes were either too small and broad or too large and sharp, respectively. This relatively remote location for the SIZ is somewhat surprising. We are currently performing experiments to locate the SIZ in living cells and testing the assumptions used in setting up the model.

The model could then be used to calculate the passive attenuation of postsynaptic potentials between any points, including this putative location of the SIZ. Our

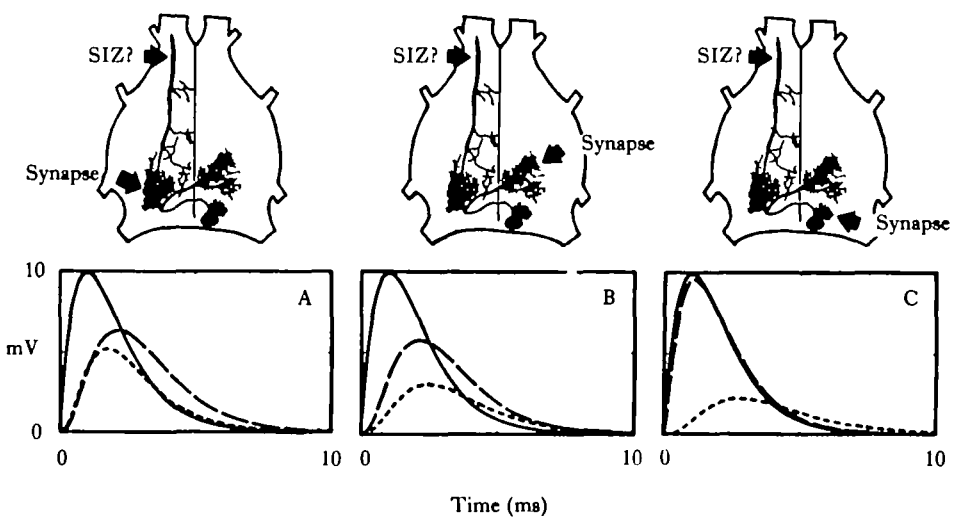

Fig. 4. EPSPs calculated at the soma (long-dashed curves) and at the spike initiating zone (short-dashed curves) due to synapses located on each of three different dendritic branches (solid curves) on a model 10-3 neurone. The *camera lucida* drawing above each panel indicates the site where the 'standard' EPSP was placed on the model cell. The putative location of the spike initiating zone (SIZ) is also indicated.

approach was (1) to generate a 'standard' 10 mV EPSP at a selected input site on the model structure and (2) to calculate what the amplitude and time course of the attenuated EPSP would be at the SIZ and at the cell body (Fig. 4). For each of three dendritic input sites, the standard EPSP is drawn with a solid line, and the resulting soma and SIZ EPSPs with a long-dashed line and a short-dashed line respectively.

First consider panel A, which shows the result of a 10 mV EPSP onto dendrite A. The peak amplitudes of the attenuated EPSPs calculated at the cell body and SIZ were 6·4 and 5·2 mV, respectively. These nearly equal attenuations are easily understood in terms of the structure of the cell: dendrite A is approximately equidistant from both the soma and SIZ. The results in panel C are also easily understood in terms of the 'electroanatomical distances' involved. A 10 mV EPSP onto dendrite C suffers little attenuation over the short path to the soma, but is severely attenuated along the long pathway to the SIZ. Peak amplitudes at the soma and SIZ were 9·6 and 2·2 mV, respectively. The centre panel shows the results of an EPSP onto dendrite B where peak EPSP amplitudes at the soma and SIZ were 5·8 and 3·1 mV, respectively. These results also make sense in light of the previous two panels: inputs onto this branch are the farthest of all three from the soma (hence the smallest soma EPSP) but are at an intermediate distance from the SIZ with respect to the other two dendrites.

What do these calculations tell us about synaptic integration in this cell? First, the relatively high membrane resistance and large diameters of the dendrites ensure that all three of the synaptic input areas are 'electrically close' to the SIZ. The attenuation between the site of synaptic input and the SIZ ranges from 48 % (for dendrite A) to 78 % (for dendrite C). Although inputs to dendrite A would therefore have a greater 'weight' in controlling spike output of the cell, inputs to C would certainly exert a substantial effect. Second, by the same reasoning, the synaptic input areas are not isolated from one another, since they are closer to one another than they are to the SIZ. Thus, any inhibitory input to one branch might cause a significant 'shunt' to current entering another branch. Finally, and most important, the soma seems to be a valid recording site for this particular neurone. Indeed, the soma is electrically 'closer' to each of the synaptic inputs than the SIZ. Even the details of the directionality plots measured at the soma should be fairly accurate representations of what the SIZ 'sees'. Table 1 shows the values of the peak amplitude of 'composite' EPSPs calculated for the soma and SIZ, for different combinations of 'standard' EPSPs onto subsets of the three branches. For ease of comparison, the results obtained by normalizing each

Table 1. *Values of the peak amplitudes of 'composite' EPSPs for different combinations of 'standard' EPSPs*

Dendrites receiving a 'standard' EPSP	Peak amplitude calculated at SIZ		Peak amplitude calculated at soma	
	mV	Normalized	mV	Normalized
ABC	10·0	1·00	19·8	1·00
AB	8·0	0·80	12·0	0·61
AC	7·1	0·71	14·5	0·73
BC	5·2	0·52	14·0	0·71
A	5·2	0·52	6·4	0·32
B	3·1	0·31	5·8	0·29
C	2·2	0·22	9·6	0·48

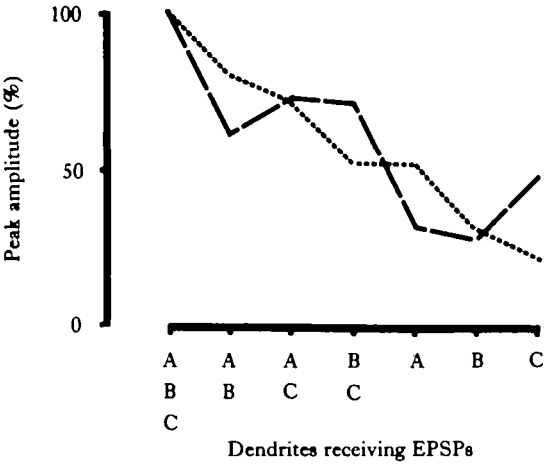

Fig. 5. Peak amplitude of composite EPSPs due to simultaneous activation of synapses onto different combinations of the three dendrites of the model 10-3 neurone. Values were calculated at the soma (long-dashed line) and the SIZ (short-dashed line). The subset of the three dendrites activated in each are listed along the x axis. Values on the y axis are expressed as percentage of the maximal amplitude for each series (obtained by simultaneous activation of all three branches).

column to its maximal value are also listed, and plotted in Fig. 5. Discrepancies between the calculated effects at the two different sites are due largely to the location of dendrite C much closer to the soma than to the SIZ.

The use of this computer model has greatly enhanced our understanding of this neurone. Modelling studies are currently in progress that should help us to understand better the experiments in which single dendrites were inactivated with the laser microbeam.

MICROSTRUCTURE AND ULTRASTRUCTURE

The above calculations serve as an illustration of the more general principle, that the location of a dendritic arbor determines the other neurones with which a neurone may interact. From a 'developmental' standpoint, a neurone must 'send its branches' to particular locations in the CNS to obtain the appropriate inputs and to deliver the appropriate outputs. Once a dendrite has grown where it is 'supposed' to go, the fine structure of that dendrite must be 'adjusted' to obtain the appropriate synaptic efficacy. The material presented in the next two sections illustrates how the 'microstructure' and 'ultrastructure' of each dendrite can determine the extent to which synaptic input at one point in the cell will influence activity at any other point.

Dendritic microstructure and synaptic efficacy

Theoretical studies over the last three decades have given us a broad understanding of the relationships between dendritic structure and function (for excellent reviews, see Rall, 1977; Jack, Noble & Tsien, 1975). Six of the most crucial biophysical parameters that influence the extent to which synaptic potentials are passively attenuated between two points along a branched dendritic structure are: (1) membrane resistivity, (2) membrane capacitance, (3) cytoplasmic resistivity, (4) distance

between the two sites, (5) diameter of the dendrite and (6) the extent of 'side branching' between the two sites. Our understanding of these factors could be simply summarized through a consideration of interneurone 10-3. Consider, from a developmental standpoint, the dendrite that was the target of the laser-ablation experiments. If our personified neurone 'wanted' to maximize the interaction between synapses on the arborizations in areas A and B, it should grow an interconnecting dendrite B with (1) the shortest and most direct route, (2) the fewest number of side branches, (3) a large diameter, (4) a high membrane resistivity and (5) a low cytoplasmic resistivity. (Here we consider the membrane capacitance to be a constant 'beyond the control' of the neurone.) Any variation from these 'rules' due to other constraints would result in a decrease in the coupling between these two regions.

With all these factors in mind, Wilfrid Rall and one of us recently realized that the dependence of synaptic efficacy upon another important factor had never been systematically investigated (Miller & Rall, 1982). That factor is total dendritic length. How would the amplitude and time course of a PSP change if the length of dendrite distal to the point of synaptic contact were increased? From our developmental perspective: how would synaptic efficacy be affected by a developmental 'overshoot' of

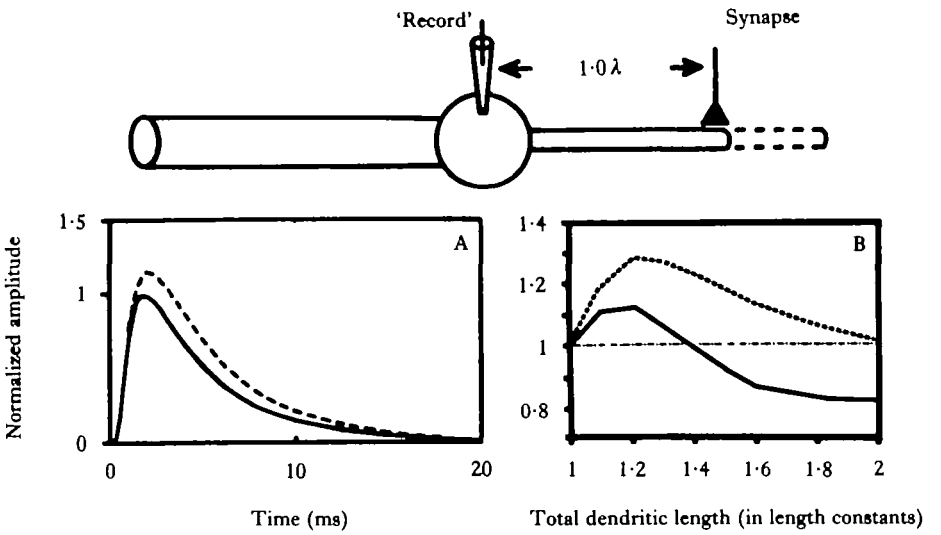

Fig. 6. Dependence of synaptic efficacy upon total dendritic length. At the top is a schematic diagram of the model neurone, which had 12 branches. For these calculations, 11 branches were lumped into one equivalent cylinder (large cylinder on left), and one single shorter branch (on the right) was contacted at its tip with a model synapse, represented as a conductance change. Model parameters: Ri = 70 Ωcm, Rm = 2500 Ωcm^2 (uniform), Cm = 2 μF cm^{-2}, Rn = 1·5 MΩ, ϱ = 10. The dashed portion of the right dendrite beyond the synapse represents the additional membrane that is 'grown on' during the theoretical 'experiment'. Panel A shows the EPSPs (i.e. voltage *vs* time) calculated in the soma due to activation of the synapse, for (1) synapse on the end of the short dendrite (solid curve); (2) 'growth' of an additional 0·2 of a length constant (λ) past the point of synaptic contact (dashed line). Time is in ms, and voltage is normalized such that the control (L = 1 λ) had a peak amplitude defined as 1 (actual amplitude was 1·6 mV). Panel B shows graphs of the data collected from several such calculations using identical synapses at the same position (1) on dendrites of varying length. Solid curve: peak PSP amplitude at soma *vs* total dendritic length, normalized to the peak amplitude of the control case (L = 1 λ). Dotted curve: charge injected onto the soma membrane *vs* total dendritic length, normalized to the charge of the control case.

the target synapse? We expected that as more dendrite was added beyond the point of synaptic contact, more synaptic current would be shunted down this extra tube and out across the extra membrane, resulting in a decrease in synaptic efficacy as measured at the soma. However, for a wide range of parameters, we obtained the opposite result: synaptic efficacy was increased by the addition of extra dendritic membrane.

This result is shown in Fig. 6. In part A, the model 'experiment' is shown diagrammatically at the top. We have used a simple 'ball and cylinder' model, with a 'recording electrode' (i.e. calculation point) in the cell body, and a synapse at the tip of the dendritic cylinder. The 'control' EPSP (calculated at the soma) due to the activation of the synaptic conductance change is shown as the solid line in panel A. Next, the dendrite is 'grown' an additional 0·2 of a length constant beyond the synapse, indicated by the dashed cylinder. The result now of activating the same synaptic conductance change is a somatic EPSP of increased amplitude and duration (dashed curve in Fig. 6A). If the dendrite 'growth' is continued, the somatic PSP begins to decrease in amplitude, until a lower asymptotic value is approached.

These results are shown graphically in Fig. 6B. The solid curve is a plot of peak PSP amplitude at the soma *versus* total dendritic length, for a synapse one length constant from the soma. The curve drawn with a dotted line is a plot of the total charge imposed on the soma membrane by the PSP *versus* the dendritic length. (This value is proportional to the area under the somatic EPSP, and is perhaps a better measure of synaptic efficacy than the peak amplitude.) Values used to plot each curve were normalized to the initial value for each. (For example, that plotted on the solid curve for a total dendritic length of $1{\cdot}2\,\lambda$ was obtained by dividing the peak amplitude of the dashed EPSP in panel A by the peak amplitude of the solid EPSP in panel A. The value plotted on the dotted curve in panel B for total $L = 1{\cdot}2\,\lambda$ was obtained by dividing the area under the dashed EPSP in panel A by the area under the solid EPSP.)

Several aspects of the curves in Fig. 6 deserve special note. First, the seemingly counter-intuitive effect is observed: that the efficacy of a synapse at a fixed location can be augmented by an increase in dendritic length beyond the point of that synaptic contact. For the parameters used here (see legend), that increase in efficacy can be a substantial 10–30%. Secondly, there is an optimum range for the total dendritic length for a synapse at a particular location (i.e. there is a 'hump' in the curves).

What could be the basis for this strange effect? The answer is simple in retrospect, and was anticipated in analytical studies by Horwitz (1981). Synaptic conductance changes are fast transients, and cause current and voltage transients that are usually much shorter in duration than the neuronal time constant. Thus, most of the current that enters a dendrite during a synaptic conductance change goes into charging the capacitance of the membrane, and 'does not have time' to leak across the membrane resistance. Thus, the functionally relevant effect of increasing the local membrane surface area (i.e. growing more dendrite) is to increase the local capacity for storing charge. More charge can get in, and the PSP measured some distance away can increase in efficacy. This effect would be observed if local membrane surface area were increased by any means, including increased infolding or varicose swellings. These effects would only be observable if single or summated conductance changes are large enough to cause local PSPs (at the site of synaptic contact) that reach a substantial percentage of the reversal potential; the weaker the synapse, the weaker the effect.

Considering the high input impedances of fine dendritic processes, however, such large amplitude local PSPs are certainly possible. For example, IPSPs can often summate effectively to 'clamp' a dendrite to the inhibitory reversal potential.

If these considerations are added to the list of 'rules' a neurone must 'keep in mind' when growing dendrites or adjusting its synaptic strengths, several interesting possibilities present themselves. For example, might the B dendrite of the cricket interneurone actually grow beyond its target synapses to optimize those interactions? If so, should we reformulate our 'general principle' of the relationship between structure and function at the macroscopic level, since the overall length and locations of terminal dendritic branches might lie beyond the 'intended' synaptic partners? Definitive answers to these complex speculative questions may be very difficult to obtain. Until we have a better understanding of (1) what cellular parameters are 'controlled' during the development or plastic change in a dendrite, and (2) how 'tightly' those parameters are controlled, we must be conservative in our estimates of the structural 'slop' of any neuronal system.

Dendritic ultrastructure and synaptic efficacy

Although most electro-anatomical studies have concentrated upon the structures at macro- and microscopic levels, one ultrastructural feature of nerve cells that has always attracted a wide interest is the dendritic spine. Dendritic spines are small 'lollipop-like' structures, consisting of an enlarged (sometimes spherical) 'head' at the tip of a thin stalk or 'neck', studding the surface of some dendrites like barbs on a cactus (Chang, 1952; Jacobsen, 1967; Jones & Powell, 1969; Peters & Kaiserman-Abramof, 1970; Ramon y Cajal, 1911; Scheibel & Scheibel, 1968). In most parts of the mammalian CNS, the majority of excitatory synapses are located on the heads of dendritic spines. Spines are also widely observed in many invertebrate preparations including the cricket cercal afferent system. Significant activity-dependent changes in the morphological parameters of spines have been reported in bees and mammalian brain slices (Brandon & Coss, 1982; Coss & Globus, 1978; Fifkova & Anderson, 1981; Fifkova & vanHarreveld, 1977; Lee, Schottler, Oliver & Lynch, 1980). Several severe neuropathologies have been shown to correlate with alterations in the density, distribution or morphology of spines (see, for example, Purpura, 1974).

What could be the functional correlate of these structures? Previous theoretical studies have shown that: (1) the efficacy of a synapse onto a spine head is different from that of the same synapse onto the 'parent' dendrite and (2) changes in the structural and electrical parameters of a spine can alter synaptic efficacy. Most of the theoretical studies were based upon the assumption that the membrane on the spine head is passive (i.e. incapable of generating an action potential). Based upon this assumption, the efficacy of a synapse onto a passive spine would always be less than, or equal to, that of a synapse directly onto the parent dendrite (Diamond, Gray & Yasargil, 1970; Kawato & Tsukahara, 1983; Koch & Poggio, 1983; Rall, 1974; Rinzel, 1982; Shepherd & Brayton, 1979; Turner & Schwartzkroin, 1983). This attenuation of a PSP by a passive spine would be due to the 'I×R drop' through the stem (the thin stem restricts the flow of current from the head into the dendrite). However, as pointed out by Rall (1978), this 'sacrifice in efficacy' might be rewarded by a 'gain in adjustability': by changing the degree of the I×R drop through the stem, the efficacy

of the EPSP might be 'adjusted' to an 'appropriate' value. Two mechanisms by which the spine stem resistance could be decreased are: (1) a decrease in stem length, and (2) an increase in stem diameter. Such considerations have led Crick (1982) to propose that spines may actually 'twitch' over a rapid time course. A temporary muscle-like 'contraction' of the spine stem would lower its resistance, decrease the I×R drop and lead to a temporary increase in synaptic efficacy. However, no such structural or electrical manipulation of a passive spine could ever yield a larger EPSP than one from a synapse placed directly onto the parent dendrite. In other words, a passive spine could, at best, be a 'variable attenuator' of synaptic input, but never an 'amplifier'.

How might this picture change if the spine head had an active instead of a passive membrane? In 1975, Jack *et al.* performed several calculations to address this question. Based upon steady-state considerations, they suggested that an active spine might actually amplify an EPSP, if the voltage in it were sufficient to bring the membrane above threshold. The regenerative current entering during the 'local' action potential in the spine head might substantially augment the synaptic current, even if the dendrite itself were not capable of generating an action potential. One of us recently participated in a study directed toward a more detailed analysis of active spines (J. P. Miller, W. Rall & J. Rinzel, in preparation). Compartmental computer models were used to calculate the voltage transients that would result from transient conductance changes onto spines with active head membranes. The models used structural parameters for spines within the range of values reported in the literature.

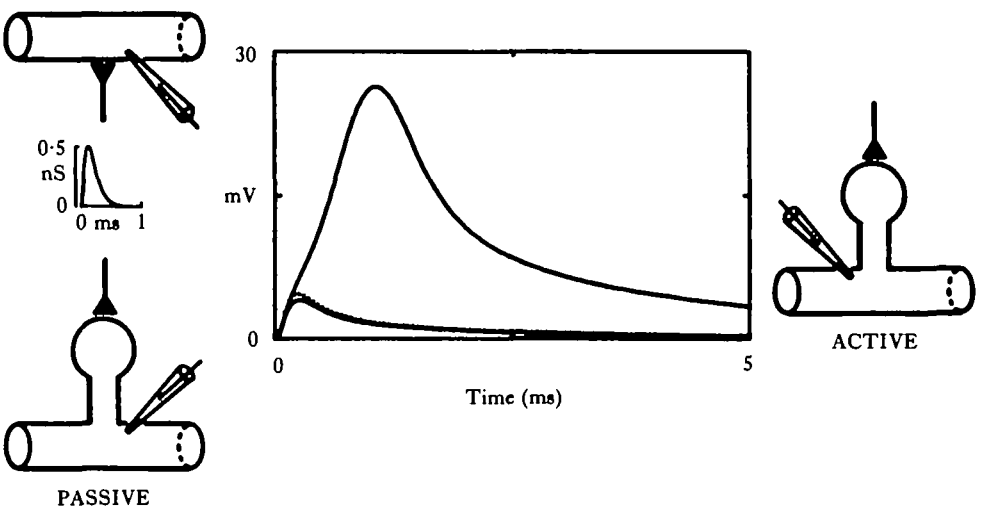

Fig. 7. Spines with active heads can greatly augment synaptic efficacy. EPSPs were calculated for identical conductance changes on three different structures: a passive dendrite (dotted curve), a passive spine onto an identical dendrite (lower solid curve) and an active spine (upper solid curve). The conductance transient is suprathreshold for action potential generation in the active head, resulting in a substantial augmentation of the current entering the spine. This results in a much enhanced EPSP at the base of the active spine. Parameters used for model calculations were as follows: resting membrane resistivity = 5000 Ωcm^2, cytoplasmic resistivity = 100 Ωcm, membrane capacitance = 1 $\mu F\,cm^{-2}$, dendrite diameter = 1 μm, dendrite length infinite, spine head diameter = 0·75 μm, spine stem resistance = 400 MΩ, synaptic conductance transient: time course proportional to $\alpha e^{-\alpha/\tau}$, $\alpha = 50$, $\tau = 5$ ms, peak conductance 0·5 nS, action potential three variable model (Rall & Shepherd, 1968): kinetic coefficients: $k_1 = 10^5$, $k_2 = 6\times10^4$, $k_3 = 25$, $k_4 = 0{\cdot}2$, $k_5 = 1$, $k_6 = 0{\cdot}01$, $k_7 = 5$, reversal potential (for active inward current, relative to rest) = 125 mV.

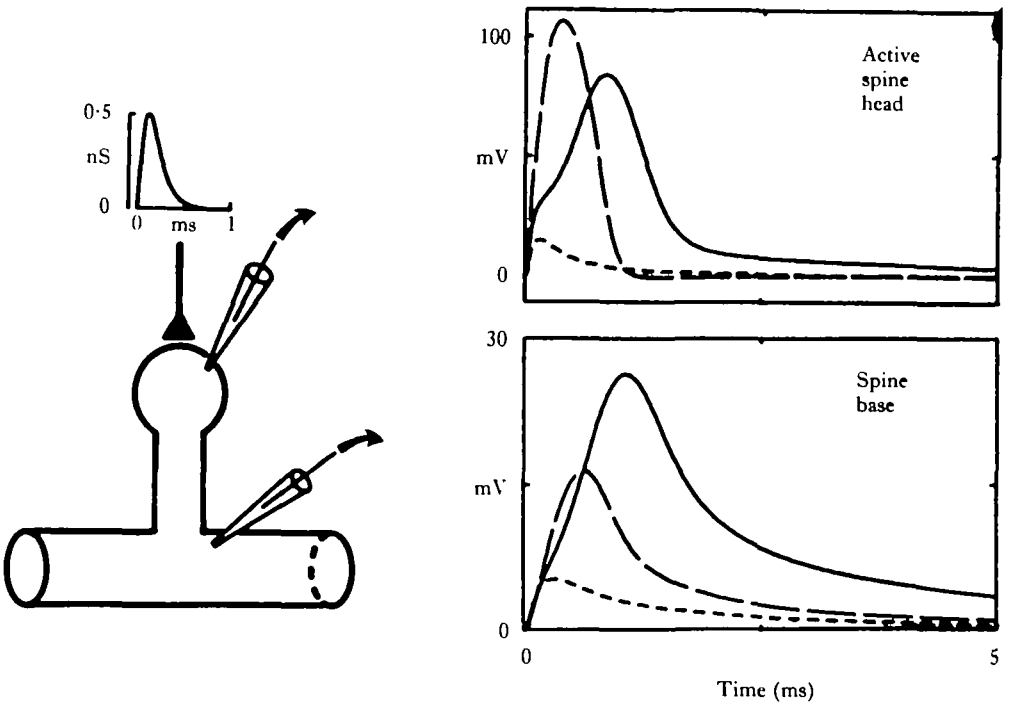

Fig. 8. There is an optimal stem resistance for maximal synaptic efficacy. The diagram on the left represents the spine model. All structural and electrical parameters of the spine and dendrite except spine stem resistance are as in Fig. 7. Directly above the spine diagram is the time course of the synaptic conductance used for all calculations; peak conductance is 0·5 nS. In each of the two enclosed panels are the voltage transients (EPSPs) corresponding to three different spine stem resistance values. EPSPs corresponding to stem resistance values of 200 MΩ, 400 MΩ and 800 MΩ are represented with short-dashed, solid, and long-dashed lines, respectively. The EPSPs were calculated at two different locations (spine head and spine base) for a spine head with active membrane. Note that the 400 MΩ stem results in a suprathreshold response for the active head (solid curve, upper right), yielding the largest PSP at the base of the spine (solid curve, lower right). Stems of either higher or lower resistances give lower amplitude EPSPs at the base.

Our results, summarized below, substantiate and extend the earlier results of Jack *et al.* (1975), and leave us with the possibility that active spines may act as relatively high-gain synaptic amplifiers. We note that D. Perkel & D. Perkel (in preparation) have addressed the same question using a slightly different approach, and have obtained essentially identical results.

We asked two specific questions. First, what would be the difference in efficacy between a synapse onto a passive and an active spine? Fig. 7 shows the EPSPs that were calculated for identical conductance transients onto three different structures: a passive dendrite, a passive spine and an active spine. (The passive electrical parameters of all three structures are identical, the physical dimensions of their dendrites were the same and the dimensions of the active and passive spines were the same.) As expected, the EPSP onto the passive spine (lower solid curve) was smaller than the EPSP directly onto a passive dendrite (dotted curve), due to the I×R drop through the passive spine stem. However, the PSP calculated at the base of the active spine was much larger, because the spine head exceeded the threshold for initiation of an action potential. The charge delivered through the spine stem into the dendrite

proportional to the area under the EPSP at the spine base) increased more than tenfold, resulting in an EPSP at the spine base that was longer and had a peak amplitude 6·5 times greater. Thus, synaptic efficacy was substantially increased.

Our second question was: how would the efficacy of a synapse onto an active spine depend upon the structural and electrical parameters of the spine? The transient computations (Fig. 8) show the effect of changing the stem resistance of an active spine, when all other parameters were left unchanged. A synaptic conductance change identical to the one used for the previous figure was initiated in the active spine head, and the resulting voltage transients were calculated both at the head and base of the spine. The solid curves in Fig. 8 are the EPSPs calculated for the 'standard' stem resistance. When this was reduced by half, a greatly reduced EPSP was obtained (curves with short dashes). This was because the reduction in stem resistance caused an overall decrease in input resistance at the spine head. The voltage transient in the head due to the conductance change was therefore reduced, and was not great enough to trigger an action potential.

When the stem resistance was doubled, the curves drawn with long dashes were obtained. The peak amplitude of the PSP in the spine head increased, but at the base was much decreased. How can this be? Doubling the stem resistance increased the input resistance of the spine head. This in turn increased the voltage response and caused the membrane to reach threshold earlier. Even though the resulting action potential in the head had a larger peak amplitude, it had a much shorter latency and duration. As a result, much less charge was delivered to the dendrite, and the resulting EPSP there had a smaller amplitude and area.

Any further increase of spine stem resistance would cause further reductions of the EPSP at the spine base, so that a maximal EPSP will occur at an intermediate spine stem resistance. This optimum corresponds to conditions where the spine head depolarization just exceeds threshold, and to an intermediate value of synaptic conductance.

Measurements of the stem resistance in real spines have not been reported in the literature. Estimates of stem resistance based upon reported ranges of stem dimensions (assuming a uniform cytoplasmic resistivity) yield values at the low end of the range used in our calculations, that may substantially underestimate the true stem resistance (Wilson, Groves, Kitai & Linder, 1983). A significant proportion of a spine stem may be occluded by extensive cytoskeletal structures and by large membrane-bound vesicles called the spine apparatus (SA) (Fifkova & Delay, 1982; Matus *et al.* 1982; Tarrant & Routtenberg, 1979; Westrum, Jones, Gray & Barron, 1980). The resistance of such partially occluded stems could certainly fall within the ranges used for these calculations. Furthermore, the resistance of occluded stems would be very sensitive to small changes in diameter of either the SA or the stem itself.

Thus, a dendritic spine could theoretically function as an EPSP amplifier, if the membrane in its head were active, and if the stem resistance and other biophysical parameters lay within the appropriate ranges. The 'gain' of the spine would be variable, and sensitive to small changes in stem resistance around an optimal value. These calculations also emphasize the importance of ultrastructural features that are 'invisible' at the light microscopic level and, therefore, are usually ignored during the 'quantitative' morphological reconstruction of neurones. Local fluctuations in the density or activity of internal structures such as the spine apparatus or cytoskeletal

meshwork might significantly alter the effective cytoplasmic resistivity, by directly obstructing the path for current or by changing the local ionic milieu. Assuming uniform cytoplasmic resistivity would lead to the same errors as arise if an 'average diameter' were used for calculations involving dendrites studded with multiple varicosities or constrictions. All of these possibilities have significant functional implications for local interactions, synaptic efficacy and plasticity, and provide an excellent demonstration of the interdependence between neuronal ultrastructure and function.

CLOSING REMARKS

We have examined the relationships between neuronal form and function as if through microscopes of successively higher power: a stereodissecting microscope, for the three dimensional structure of whole cricket neurones, a compound microscope, for synapses onto a single dendrite, and an electron microscope, for the ultrastructure of single dendritic spines. In doing so, we have attempted to show how the application of computer models and new experimental techniques have increased our knowledge in two fundamental ways: (1) we understand several aspects of neuronal integration more quantitatively, and (2) several new insights into neuronal integrative phenomena have been realized.

We acknowledge Wil Rall, John Rinzel and Rod Murphey as collaborators in the original studies and thank Barry Bunow for assistance with development of computer programmes. This work was supported in part by NSF Grant BNS-8202416 and a Sloan Foundation Fellowship to JPM, and NSF Grant BNS-8119799 to R. K. Murphey.

REFERENCES

BACON, J. P. & ALTMAN, J. S. (1977). A silver intensification method for cobalt filled neurons in wholemount preparations. *Brain Res.* **138**, 359–363.

BACON, J. P. & MURPHEY, R. K. (1984). Receptive fields of cricket giant interneurons are determined by their dendritic structure. *J. Physiol., Lond.* (in press).

BRANDON, J. G. & COSS, R. G. (1982). Rapid dendritic spine stem shortening during one-trial learning: the honeybee's first orientation flight. *Brain Res.* **252**, 51–61.

CHANG, H. T. (1952). Cortical neurons with particular reference to the apical dendrites. *Cold Spring Harb. Symp. quant. Biol.* **17**, 189–202.

COSS, R. G. & GLOBUS, A. (1978). Spine stems on tectal interneurons in jewel fish are shortened by social stimulation. *Science, N.Y.* **200**, 787–789.

CRICK, F. (1982). Do dendritic spines twitch? *Trends Neurosci.* **5**, 44–46.

DIAMOND, J., GRAY, E. J. & YASARGIL, G. M. (1970). The function of the dendritic spine: an hypothesis. In *Excitatory Synaptic Mechanisms*, (eds P. Anderson & J. K. S. Jansen), pp. 213–222. Oslo: Universitetsforlaget.

FIFKOVA, E. & ANDERSON, C. L. (1981). Stimulation induced changes in dimensions of stalks of dendritic spines in the dentate molecular layer. *Exp. Neurol.* **74**, 621–627.

FIFKOVA, E. & DELAY, R. J. (1982). Cytoplasmic actin in neuronal processes as a possible mediator of synaptic plasticity. *J. Cell Biol.* **95**, 345–350.

FIFKOVA, E. & VANHARREVELD, A. (1977). Long-lasting morphological changes in dendritic spines of dentate granule cells following stimulation of the entorrhinal area. *J. Neurocytol.* **6**, 211–230.

HORWITZ, B. (1981). Neuronal plasticity: how changes in dendritic architecture can effect the spread of postsynaptic potentials. *Brain Res.* **224**, 412–418.

JACK, J. J. B., NOBLE, D. & TSIEN, R. W. (1975). *Electrical Current Flow in Excitable Cells*. Oxford: Clarendon Press. pp. 222–223.

JACOBSEN, S. (1967). Dimensions of the dendritic spine in the sensorimotor cortex of the rat, cat, squirrel, monkey and man. *J. comp. Neurol.* **129**, 49–58.

JONES, E. G. & POWELL, T. P. S. (1969). Morphological variations in the dendritic spines of the neocortex. *J. Cell Sci.* **5**, 509–529.

KAWATO, M. & TSUKAHARA, N. (1983). Theoretical study on electrical properties of dendritic spines. *J. theor. Biol.* **103**, 507–522.

KOCH, C. & POGGIO, T. (1983). A theoretical analysis of electrical properties of spines. *Proc. R. Soc. B* **218**, 455–477.

LEE, K. S., SCHOTTLER, F., OLIVER, M. & LYNCH, G. (1980). Brief bursts of high frequency stimulation produce two types of structural change in rat hippocampus. *J. Neurophysiol.* **44**, 247–258.

LEVINE, R. B. & MURPHEY, R. K. (1980). Pre- and postsynaptic inhibition of identified giant interneurons in the cricket (*Acheta domesticus*). *J. comp. Physiol.* **135**, 269–282.

LEV-TOV, A., MILLER, J. P., BURKE, R. E. & RALL, W. (1983). Factors that control amplitude of EPSPs in dendritic neurons. *J. Neurophysiol.* **50**, 399–412.

MATUS, A., ACKERMAN, M., PEHLING, G., BYERS, H. R. & FUJIWARA, K. (1982). High actin concentrations in brain dendritic spines and postsynaptic densities. *Proc. natn. Acad. Sci. U.S.A.* **70**, 7590–7594.

MILLER, J. P. & RALL, W. (1982). Effect of dendritic length upon synaptic efficacy. *Neurosci. Abst.* **8**, 414.

MILLER, J. P. & SELVERSTON, A. I. (1979). Rapid killing of single neurons by irradiation of intracellularly injected dye. *Science, N.Y.* **185**, 181–183.

MURPHEY, R. K., WALTHALL, W. W. & JACOBS, G. A. (1984). Neurospecificity in the cricket cercal system. *J. exp. Biol.* **112**, 7–25.

PALKA, J., LEVINE, R. & SCHUBIGER, M. (1977). The cercus-to-giant interneuron system of crickets. I. Some attributes of the sensory cells. *J. comp. Physiol.* **119**, 267–283.

PETERS, A. & KAISERMAN-ABRAMOF, I. R. (1970). The small pyramidal neuron of the rat cerebral cortex. The perikaryon, dendrites and spines. *Am. J. Anat.* **127**, 321–356.

PURPURA, D. P. (1974). Dendritic spine dysgenesis and mental retardation. *Science, N.Y.* **186**, 1126–1128.

RALL, W. (1974). Dendritic spines, synaptic potency and neuronal plasticity. In *Cellular Mechanisms Subserving Changes in Neuronal Activity*, (eds C. D. Woody, K. A. Brown, T. J. Crow, Jr. & J. D. Knispel), pp. 13–21. Brain Inf. Serv. Res. Rpt. No. 3, UCLA Press.

RALL, W. (1977). Core conductor theory and cable properties of neurons. In *Handbook of Physiology. The Nervous System I*, (ed. E. Kandel), pp. 39–97. Bethesda, Md.: American Physiological Society.

RALL, W. (1978). Dendritic spines and synaptic potency. In *Studies in Neurophysiology*, (ed. R. Porter), pp. 203–209. Cambridge: Cambridge University Press.

RALL, W. & SHEPHERD, G. M. (1968). Theoretical reconstruction of field potentials and dendrodendritic synaptic interactions in olfactory bulb. *J. Neurophysiol.* **31**, 884–915.

RAMON Y CAJAL, S. (1911). *Histologie du Syteme Nerveaux de l'Homme et des Vertebres*, Vols 1 & 2. Paris: A. Maloine.

REICHERT, H., PLUMMER, M. R. & WINE, J. J. (1983). Identified nonspiking local interneurons mediate non-recurrent, lateral inhibition of crayfish mechanosensory interneurons. *J. comp. Physiol.* **151**, 261–276.

RINZEL, J. (1982). Neuronal plasticity (learning). *Lectures on Mathematics in the Life Sciences* **15**, 7–25.

SCHEIBEL, M. E. & SCHEIBEL, A. B. (1968). On the nature of dendritic spines – report of a workshop. *Communs Behav. Biol.* 1A, 231–265.

SHEPHERD, G. M. & BRAYTON, R. K. (1979). Computer simulation of a dendrodendritic synaptic circuit for self- and lateral-inhibition in the olfactory bulb. *Brain. Res.* **175**, 377–382.

TARRANT, S. B. & ROUTTENBERG, A. (1979). Postsynaptic membrane and spine apparatus: proximity in dendritic spines. *Neurosci. Lett.* **11**, 289–294.

TOBIAS, M. & MURPHEY, R. K. (1979). The response of cercal receptors and identified interneurons in the cricket (*Acheta domesticus*) to air streams. *J. comp. Physiol.* **129**, 51–59.

TURNER, D. A. & SCHWARTZKROIN, P. A. (1983). Electrical characteristics of dendrites and dendritic spines in intracellularly stained CA3 and dentate hippocampal neurons. *J. Neurosci.* **3**, 2381–2394.

WESTRUM, L. E., JONES, H. D., GRAY, E. G. & BARRON, J. (1980). Microtubules, dendritic spines and spine apparatuses. *Cell Tiss. Res.* **208**, 171–181.

WILSON, C. J., GROVES, P. M., KITAI, S. T. & LINDER, J. L. (1983). Three dimensional structure of dendritic spines in the rat neostriatum. *J. Neurosci.* **3**, 383–398.